Published in final edited form as:
Cancer Biol Ther. 2009 October ; 8(20): 1962–1971.

Mitochondrial ROS and radiation induced transformation in mouse embryonic fibroblasts

Changbin Du,
Free Radical and Radiation Biology Program, Department of Radiation Oncology, University of Iowa, Iowa City, Iowa

Zhen Gao,
Nevada Cancer Center, Los Vegas, Nevada

Venkatasubbaiah A. Venkatesha,
Free Radical and Radiation Biology Program, Department of Radiation Oncology, University of Iowa, Iowa City, Iowa

Amanda L. Kalen,
Free Radical and Radiation Biology Program, Department of Radiation Oncology, University of Iowa, Iowa City, Iowa

Leena Chaudhuri,
Free Radical and Radiation Biology Program, Department of Radiation Oncology, University of Iowa, Iowa City, Iowa

Douglas R. Spitz,
Free Radical and Radiation Biology Program, Department of Radiation Oncology, University of Iowa, Iowa City, Iowa

Joseph J. Cullen,
Free Radical and Radiation Biology Program, Department of Radiation Oncology, University of Iowa, Iowa City, Iowa

Larry W. Oberley, and
Free Radical and Radiation Biology Program, Department of Radiation Oncology, University of Iowa, Iowa City, Iowa

Prabhat C. Goswami
Free Radical and Radiation Biology Program, Department of Radiation Oncology, University of Iowa, Iowa City, Iowa

Abstract

Manganese superoxide dismutase (SOD2) is a nuclear encoded and mitochondria localized antioxidant enzyme that converts mitochondria derived superoxide to hydrogen peroxide. This study investigates the hypothesis that mitochondria derived reactive oxygen species (ROS) regulate ionizing radiation (IR) induced transformation in normal cells. Mouse embryonic fibroblasts (MEFs) with wild type SOD2 (+/+), heterozygous SOD2 (+/−), and homozygous SOD2 (−/−) genotypes were irradiated with equitoxic doses of IR, and assayed for transformation frequency, cellular redox

Corresponding Author: Prabhat C. Goswami, PhD, Free Radical and Radiation Biology Program, Department of Radiation Oncology, B180 Medical Laboratories, University of Iowa, Iowa City, IA-52242. Phone: (319) 384-4666, Fax: (319) 335-8039, prabhat-goswami@uiowa.edu.

We dedicate this manuscript in honor and memory of the late Dr. Larry W. Oberley

There is no conflict of interest.

environment, DNA damage, and cell cycle checkpoint activation. Transformation frequency increased (~ 5-fold) in SOD2 (−/−) compared to SOD2 (+/+) MEFs. Cellular redox environment (GSH, GSSG, DHE, and DCFH-oxidation) did not show any significant change within 24h post-IR. However, a significant increase in cellular ROS levels was observed at 72h post-IR in SOD2 (−/−) compared to SOD2 (+/+) MEFs, which was consistent with an increase in GSSG in SOD2 (−/−) MEFs. Late ROS accumulation was associated with an increase in micronuclei frequency in SOD2 (−/−) MEFs. Exit from G_2 was accelerated in irradiated SOD2 (+/−) and SOD2 (−/−) compared to SOD2 (+/+) MEFs. These results support the hypothesis that SOD2 activity and mitochondria generated ROS regulate IR induced transformation in mouse embryonic fibroblasts.

Keywords

SOD2; mitochondria; ROS; radiation; transformation; micronuclei; γ-H2AX; G_2-checkpoint

INTRODUCTION

Cellular redox environment is a balance between production of ROS ($O_2^{\bullet-}$ and H_2O_2) and their removal by antioxidants. Superoxide is converted to H_2O_2 by superoxide dismutase enzymes (CuZnSOD: SOD1; MnSOD: SOD2; and EcSOD: SOD3), while catalase and glutathione peroxidases neutralize H_2O_2. SOD2 is a nuclear encoded and mitochondria localized homo-tetramer (88 kDa) that is known to convert mitochondria generated $O_2^{\bullet-}$ to H_2O_2. ROS can be generated both from endogenous sources (mitochondrial electron transport chain and oxygen metabolizing enzymes) and exogenous sources (e.g. ionizing radiation). Ionizing radiation (IR) results in oxidative stress both by direct transfer of photons and indirectly by radiolysis of water[1–3].

Pre-treatment with small molecular weight antioxidants and antioxidant enzymes have been reported to reverse IR induced cytotoxicity[4–8]. IR-induced changes in cellular antioxidant capacity are also known to influence cytotoxicity[9–11]. Thus, it is commonly believed that the initial changes in cellular ROS levels immediately following the radiation exposure regulate all of the subsequent cellular effects. Because the IR-induced increase in cellular ROS levels are still significantly lower compared to ROS resulted from normal metabolism[12], it is hypothesized that the initial increase in ROS levels immediately following the radiation exposure may not be the only mechanism regulating the biological effects. This hypothesis is supported by results demonstrating that antioxidants administered long after the beam is turned off significantly inhibited IR induced cytotoxicity[5, 7, 13]. Consistent with these results, we have shown previously that suppression of IR induced late ROS accumulation in SOD1 overexpressing human glioma cells correlated with radioresistance[14]. Overall, these results led to the hypothesis that the late ROS accumulation due to changes in cellular metabolism could be an additional mechanism regulating cellular responses to IR exposures[15].

The first report of SOD2 activity being different in transformed cells compared to their corresponding normal cells dates back to 1974 when Yamanaka and Deamer reported a significant decrease in SOD2 activity in SV40 transformed WI38 human lung fibroblasts compared to wild type cells[16]. The role of superoxide dismutase in cancer was eloquently addressed by Oberley and Buettner in their seminal paper published in 1979[17]. Subsequently, numerous studies report that cancer cells have lower SOD2 activity compared to their corresponding normal cells, and overexpression of SOD2 suppresses cancer cells growth *in vitro* and tumor xenografts *in vivo*[18–22]. These results support the hypothesis that SOD2 could be a tumor suppressor gene[23].

We have shown previously that overexpression of SOD2 results in radioresistance in human oral squamous cancer cells[6]. Radiation is well known to damage cellular macromolecules and activate cell cycle checkpoint pathways allowing cells enough time to repair the damage. The frequency of micronuclei and phosphorylated histone H2AX (γH2AX) levels are two of the most commonly used markers of DNA damage[24–28]. DNA damage induces acentric chromosome fragments that may result in the formation of micronuclei during cell division. H2AX is a member of the histone 2A family of proteins. Following IR exposure, H2AX is phosphorylated at Ser139 by ataxia telangiectasia mutant (ATM)[27]. In general, the kinetics of the phosphorylation and dephosphorylation of H2AX correlate with radiosensitivity. Therefore, γH2AX levels are commonly used as a predictive marker for cellular responses to DNA damage[27, 29]. Our previously published results showed that SOD activity influences cell cycle checkpoint activation in irradiated human oral squamous, pancreatic, and glioma cells[6, 14, 30], suggesting that ROS-signaling pathways could regulate cell cycle processes following DNA damage.

In this study, we used wild type SOD2 (+/+), heterozygous SOD2 (+/−), and homozygous knockout SOD2 (−/−) MEFs to determine if SOD2 activity and therefore, mitochondria generated ROS regulate IR induced cellular transformation. IR induced transformation frequency increased in SOD2 (−/−) MEFs, which was associated with a late ROS accumulation, DNA damage, and accelerated exit from G_2-phase.

MATERIALS AND METHODS

Cell culture

SOD2 (+/+) wild type, SOD2 (+/−) heterozygous, and SOD2 (−/−) homozygous knockout mouse embryonic fibroblasts (MEFs) primary cultures were generously provided by Dr. T. T. Huang (Stanford University). Cells were routinely cultured in DMEM supplemented with 10% fetal bovine serum and antibiotics following our previously published protocol[31]. Cells were grown at 37°C in a humidified incubator with 5% carbon dioxide and 4% oxygen. Plating efficiency (PE) was measured by plating MEFs on top of hamster fibroblasts that were irradiated with 30 Gy, which served as feeder cells. PE was calculated using the following formula: PE = (number of colonies counted/number of cells seeded) × 100.

Clonogenic assay

Monolayer cultures of exponentially growing control and irradiated MEFs were trypsinized, diluted, and re-plated on top of 30 Gy irradiated hamster fibroblasts feeder cells. Cells were cultured for 15 d and stained with 0.8% coomassie blue G250 in 50% methanol and 20% acetic acid. Colonies greater than or equal to 50 cells were counted as survivors; surviving fraction (SF) = (number of colonies counted)/(number of cells seeded × PE). The University of Iowa Holden Comprehensive Cancer Center Radiation and Free Radical Research Core facility resources were used for all radiation related experiments. Exponentially growing asynchronous cultures were irradiated using a cesium-137 source set at a dose rate of 0.83 Gy/min.

Transformation assay

Clonogenic MEFs were seeded in 15 T-75 flasks containing monolayer of 30 Gy irradiated hamster fibroblasts serving as feeder cells. MEFs were irradiated 24 h post-plating. The medium was changed once per week for 6 weeks. The monolayer cells were fixed with 100% methanol and stained with Giemsa stain (1:6 dilution of 0.742% w/v). The transformed state in the fibroblasts is expressed phenotypically by the appearance of morphologically distinct colonies (foci). The scoring criteria for foci set by Reznikoff *et al.*[32] were used to identify and count foci. In this study, the type II and type III foci were scored, and the transformation frequency (TF) was calculated as the number of foci per surviving cell[33].

Adenoviral infection

Replication deficient adenovirus carrying cytomegalovirus (CMV) promoter driven mouse wild type SOD2 cDNA (AdSOD2) and vector alone control (AdEmpty) were purchased from Viraquest Inc. (North Liberty, IA). Adenovirus infections were carried out following our previously published protocols[31, 34]. Monolayer cultures of SOD2 (−/−) MEFs were infected with adenovirus for 24 h in serum-free media followed by addition of regular media containing 10% FBS. Forty eight hours post-infection, cells were prepared for the transformation assay as described above.

Antioxidant enzyme and GSH assays

SOD enzymatic activities were determined following our previously published protocol[31, 34]. Control and irradiated asynchronous cultures were lysed by sonication, and 100 microgram of total cellular protein was separated by native polyacrylamide gel electrophoresis. SOD activity was visualized by incubating the gel with nitroblue tetrazolium, riboflavin, and TEMED. The activity of SOD2 and SOD1 was distinguished by adding sodium cyanide to the incubation buffer. Band intensities were quantified by AlphaImager 2000 (Alpha Innotech).

Total glutathione (GSH) and glutathione disulfide (GSSG) levels were assayed by following the previously published method of Griffith[35] in the Radiation and Free Radical Research Core at the University of Iowa. All measurements were normalized to the protein content of whole cell homogenate.

DNA damage assays

Micronuclei (MN) formation and immunoreactive phosphorylated H2AX (γH2AX, see below) levels were measured to evaluate DNA damage in control and irradiated MEFs following our previously published protocols[28]. Briefly, control and irradiated MEFs were incubated with medium containing cytochalasin-B (4 μg mL^{-1}) and harvested at 48 h post-irradiation. Methanol and acetic acid fixed cells were stained with acridine orange and visualized under a fluorescent microscope (Olympus BX-51). The frequency of micronucleated bi-nucleate cells (MNBNC) was calculated by examining four hundred bi-nucleated cells[28, 36].

Immunoblotting assay

Total cellular protein extracts were separated by SDS-PAGE and transferred onto a nitrocellulose membrane. The membrane was then incubated with antibodies to SOD2, γH2AX, and actin. An enhanced chemiluminescence kit (GE Healthcare) was used to visualize the immunoreactive polypeptides, and results were quantified using AlphaImager 2000 (Alpha Innotech). Results were calculated by first normalizing band intensities to actin levels in individual samples, and fold change calculated relative to untreated control.

Flow cytometry assays: DNA content

The DNA content was assayed following our previously published protocol[14]. Briefly, control and irradiated MEFs were fixed in 70% ethanol, washed with phosphate buffered saline and incubated with RNase A (0.1 mg mL^{-1}). At the end of 30 min incubation, propidium iodide (35 μg mL^{-1}) was added and the incubation was continued for an hour. FACScan (Becton Dickinson) and MODFIT software (Verity Software House) were used to identify and calculate the percentage of cells with G_1, S, and G_2 DNA content.

Cellular ROS levels

Monolayer cultures were incubated with Hanks buffer salt solution (HBSS) containing 10 μM dihydroethidine (DHE, Invitrogen) for 45 min or 1 μg mL^{-1} of 5-(and-6)-carboxy-2′,7′-dichlorodihydrofluorescein diacetate (DCFH-DA, Invitrogen) for 15 min at 37°C. Cells were

harvested by trypsinization, centrifuged, and re-suspended in HBSS buffer supplemented with 10% FBS. The flow cytometry measurements of DHE-oxidation were performed using 488 nm excitation and 585/42 nm band pass emission filter. The DCFH-oxidation was measured using 488 nm excitation and 530/30 nm band pass emission filter. Results from 10,000 events were collected in the list mode. The Cell Quest software (Becton Dickinson) was used to calculate the geometric mean fluorescence. Cells incubated with the buffer alone were included for autofluorescence correction[14, 30, 31].

Statistical Analysis

Statistical analysis was done using the one and two-way analysis of variance followed by Dunnett's t test. Two sample t test was used for mean comparison between two groups. Results from at least $n \geq 3$ with $p < 0.05$ were considered significant. All statistical analysis was performed using SAS 9.1.

RESULTS

SOD2 activity modulates radiation induced transformation frequency

Initially, we determined whether changes in SOD2 activity affect cellular redox environment and plating efficiency (Figure 1). Exponentially growing asynchronous cultures of MEFs were harvested and total cellular protein extracts were used for measurements of antioxidant enzyme protein levels and activity. As expected, SOD2 (+/+) MEFs demonstrated the highest protein levels and activity; SOD2 (+/−) MEFs exhibited lower levels than SOD2 (+/+), and a complete absence of SOD2 protein and activity was observed in SOD2 (−/−) MEFs (Figure 1A). Flow cytometry measurements of DHE-oxidation showed approximately 1.5-fold and 3-fold increases in SOD2 (+/−) and SOD2 (−/−) compared to SOD2 (+/+) MEFs (Figure 1B), indicating that loss of SOD2 activity increased cellular ROS ($O_2^{\bullet -}$) steady state levels. Changes in DCFH-oxidation was approximately 2-fold higher in SOD2 (−/−) compared to SOD2 (+/+) MEFs (Figure 1C). Consistent with these results, total GSH levels in SOD2 (−/−) MEFs were found to be 16 ± 2 nmoles/mg protein compared to 10 ± 2 nmoles/mg protein in SOD2 (+/+) MEFs. SOD2 activity related changes in cellular ROS levels exhibited corresponding alterations in plating efficiencies (Figure 1D): SOD2 (+/+) had the highest PE of 26 ± 7%; SOD2 (+/−), 6 ± 3%, and SOD2 (−/−) MEFs 4 ± 1%.

A clonogenic assay was performed to determine the equitoxic doses of ionizing radiation (IR) that are needed for the *in vitro* transformation assay. The radiation doses for 10% survival (equitoxic dose) were calculated to be 6.8 Gy for SOD2 (+/+), 4.4 Gy for SOD2 (+/−), and 5.6 Gy for SOD2 (−/−) MEFs. The increase dose for a 10% survival in SOD2 (−/−) MEFs compared to SOD2 (+/−) MEFs could be due to an adaptive response in SOD2 (−/−) MEFs. SOD2 (−/−) MEFs have a higher steady state levels of ROS compared to SOD2 (+/−) MEFs. The increase in the endogenous ROS levels may activate an adaptive response in SOD2 (−/−) MEFs, which could account for the higher dose that are needed to achieve the same survival response as compared to the SOD2 (+/−) MEFs. The dose for a 10% survival was selected based on a previous report in the literature[37]. The authors showed that a 10% survival dose is optimal for studying *in vitro* transformation of normal fibroblasts.

MEFs were layered on top of feeder cells, and irradiated with equitoxic doses of IR at 24 h post-plating. Control and irradiated monolayer cultures were continued in culture with regular change in media for 6–8 weeks. Identification and scoring of the transformed foci were performed following the scoring-criteria that were originally proposed by Reznikoff *et al*.[32], and Fenech *et al*.[36]. The basic criteria for Type III foci are dense multilayer cells, random cell orientation at any part of the foci edge, and invasion into the surrounding contact inhibited monolayer. Type II foci were distinguished from Type III foci primarily by their more defined

edges, and they were less dense than Type III foci. Previous reports have shown that cells representing Type II and III foci are fully transformed, and they form tumors in animals[38, 39]. Representative Type II and III foci are shown in Figure 2A. Type II and III foci were highest (~5-fold) in SOD2 (−/−) compared to SOD2 (+/+) MEFs; SOD2 (+/−) showed an intermediate response (Table 1). The transformation frequency (TF) for Type II and III foci correlated with SOD2 activity (Figure 2, Table 1, Figure 1A). These results indicate SOD2 activity, therefore mitochondria derived ROS, regulates IR induced cellular transformation in MEFs.

SOD2 activity suppressed radiation induced late ROS accumulation

In recent years, cellular redox environment is believed to be a major regulator of numerous cellular processes. A flow cytometry assay was used to measure cellular ROS levels following our previously published protocol[31]. Asynchronous monolayer cultures of control and irradiated (5 Gy) MEFs were harvested at 24 and 72 h post-IR; cells were incubated with DHE (or DCFH-DA) and fluorescence measured by flow cytometry. Results were calculated relative to time matched un-irradiated controls for each cell type. At 24 h post-IR, there was no significant difference in DHE-oxidation among the cell types compared to their un-irradiated time matched controls (Figure 3A). Interestingly, at 72 h post-IR DHE-oxidation increased approximately 1.3-fold in SOD2 (+/+) and 2.5-fold in SOD2 (−/−) MEFs ($p<0.05$). DHE-oxidation in SOD2 (+/−) MEFs did not show any difference at 72 h compared to 24 h post-IR.

Cellular ROS levels were further evaluated by measuring DCFH-fluorescence. At 24 h post-IR, all three cell types exhibited modest increase (1.2–1.6 fold) in DCFH-oxidation compared to their time matched un-irradiated controls (Figure 3B). At 72 h post-IR, DCFH-oxidation in SOD2 (+/+) MEFs was comparable to 24 h post-IR. However, both SOD2 (+/−) and SOD2 (−/−) MEFs exhibited approximately 1.4–1.8 fold increase in DCFH-oxidation at 72 h post-IR (Figure 3B). Consistent with these results, total GSH levels in SOD2 (+/−) and SOD2 (−/−) MEFs showed a small increase at 24 h compared to 72 h post-IR (Figure 3C). GSSG levels remained significantly higher at 72 h post-IR in SOD2 (−/−) compared to SOD2 (+/+) and SOD2 (+/−) MEFs (Figure 3D). These results indicate that while SOD2 activity might not influence cellular redox environment within 24 h of IR-exposure, at 72 h post-IR SOD2 activity protects cellular redox environment from shifting towards a more oxidizing environment characterized by greater steady-state ROS levels.

SOD2 activity suppressed radiation induced late DNA damage

IR is well known to cause DNA damage both by direct and indirect actions[1]. To determine if SOD2 activity influences IR-induced DNA damage, a micronuclei (MN) assay was performed. Asynchronous cell population was irradiated with 5 Gy, and cytokinesis was blocked by adding cytochalasin B at 24 h (or 72 h) post-IR. Forty eight hours after the addition of cytochalasin B, control and irradiated cells were processed for MN assay. Representative microscopy fields of MN and nucleoplasmic bridge (NPB) are shown in Figure 4A. Four hundred cells per treatment were examined for MN and NPB, and the percentage of total micronuclei bearing bi-nucleated cells (MNBNCs) were calculated (Figure 4B); the distributions of MN and NPB are summarized in Table 2. The percentage of MN in un-irradiated controls was not significantly different among the three cell types (Table 2). At 24 h post-IR, the percentage of MN significantly increased in all cell types: 46 ± 4% in SOD2 (+/+), 52 ± 9% in SOD2 (+/−), and 57 ± 9% in SOD2 (−/−) MEFs (Figure 4B and Table 2). At 72 h post-IR, significant difference was noted among the three cell types. Both SOD2 (+/+) and SOD2 (+/−) MEFs exhibited a decrease in the percentage of MNBNCs at 72 h compared to 24 h post-IR: 29 ± 5% *vs.* 46 ± 4%, and 40 ± 5% *vs.* 52 ± 9%, respectively (Table 2). Interestingly, the percentage of MNBNCs in SOD2 (−/−) MEFs remained higher (65 ± 3%) at 72 h post-IR (Table 2).

The lack of SOD2 activity influencing the early (24 h post-IR) DNA damage response is further evident from the results of phosphorylated histone H2AX (γ-H2AX) levels that were measured within 60 min post-IR (Figure 4C). γ-H2AX is one of the earliest cellular responses to IR-induced DNA damage. Asynchronous cell populations were irradiated (5 Gy), and total cellular protein extracts were analyzed at indicated time for γ-H2AX levels by immunoblotting. The basal levels of γ-H2AX in all three cell types were low. IR-exposure significantly increased γ-H2AX at 30 min post-IR in all three cell types followed by a comparable decrease at 60 min post-IR (Figure 4C). These results showed that SOD2 activity might not influence radiation induced initial DNA damage. However, increased ROS accumulation (Figure 3) and percentage of MNBNCs (Figure 4B, Table 2) at 72 h post-IR suggest that SOD2 activity could significantly impact late DNA damage and IR induced transformation.

SOD2 activity and exit from G_2 in irradiated MEFs

Cell cycle checkpoints are pivotal mechanisms safeguarding genome integrity. Cells that harbor defects in checkpoints are predisposed to genomic instability and transformation[40–42]. In order to determine if SOD2 activity could influence IR induced checkpoint activation, asynchronous cell populations of MEFs were irradiated with 5 Gy and cell cycle phase distributions assayed by flow cytometry measurements of DNA content following our previously published method[31, 34]. Representative DNA histograms are shown in Figure 5A, and the fold-change in G_2 calculated relative to 0 h un-irradiated control for each cell type (Figure 5B). While the activation of G_1 (data not shown) and G_2 checkpoints were comparable among the three cell types, interesting results were observed for cells exiting G_2 (Figure 5B). As anticipated, the fold-change in G_2 increased at 8 h post-IR for all cell types; the fold-change in SOD2 (−/−) is slightly lower compared to SOD2 (+/+) and SOD2 (+/−) MEFs at 8 h post-IR. Interestingly, at 24 h post-IR the fold-change in G_2 was lower in SOD2 (+/−) and SOD2 (−/−) compared to SOD2 (+/+) MEFs, suggesting that SOD2 activity could regulate exit from G_2 in irradiated MEFs. It is hypothesized that an accelerated exit from G_2 following IR-exposure may increase the chances of passing on cellular damage to daughter generations, which could facilitate cellular transformation.

To further determine if SOD2 activity could influence exit from G_2 in irradiated cells, SOD2 (−/−) MEFs were infected with adenovirus containing vector control (AdEmpty), and mouse SOD2 cDNA (AdSOD2). Cells were irradiated with 5 Gy and cell cycle phase distributions measured at the time of radiation, and 8 and 24 h post-IR; fold-change calculated relative to 0 h un-irradiated control for individual treatments. The fold-change in G_2 increased approximately 2-fold in AdEmpty infected SOD2 (−/−) MEFs (20 ± 2 *vs.*10 ± 1%), and 2.5-fold in AdSOD2 infected cells (26 ± 1 *vs.* 10 ± 1%) at 8 h post-IR. Interestingly, at 24 h post-IR exit from G_2 was delayed in AdSOD2 infected cells compared to AdEmpty infected cells (Figure 5C). These results were comparable to SOD2 (+/+) MEFs (Figure 5B), indicating that SOD2 activity could regulate exit from G_2 in irradiated MEFs.

DISCUSSION

Manganese superoxide dismutase (SOD2) is a nuclear encoded and mitochondria localized antioxidant enzyme known to convert mitochondria generated $O_2^{\bullet-}$ to H_2O_2. The present study was designed to determine whether SOD2 activity, and therefore mitochondria generated ROS regulate ionizing radiation (IR) induced normal cell transformation. Mouse embryonic fibroblasts (MEFs) carrying wild type (+/+), heterozygous (+/−) and homozygous knockout (−/−) SOD2 were irradiated with equitoxic doses of IR (dose rate, 0.83 Gy/min) and assayed for cellular transformation by measuring Type II and III foci. The transformation frequency was approximately 5-fold higher in SOD2 (−/−) compared to SOD2 (+/+) MEFs (Figure 2, Table 1); SOD2 (+/−) showed an intermediate response. These results are consistent with

earlier reports in the literature demonstrating SOD2 overexpression protecting cells from carcinogen induced transformation[8, 43]. Furthermore, these results also provide a direct evidence for the original hypothesis of SOD2 activity and carcinogenesis proposed by Oberley and Buettner[17].

Since SOD2 activity is known to convert mitochondria generated $O_2^{\bullet -}$ to H_2O_2, results from the transformation assay also suggest that mitochondrial ROS could influence cellular transformation in irradiated cells. Irradiation is a classical generator of ROS that persist for milliseconds and result in oxidative damage to cellular macromolecules[12]. It has been hypothesized that ROS mediated covalent modifications of cellular macromolecules could regulate some aspects of the cellular responses to IR exposure. This hypothesis is based on the observations that ROS scavengers suppress many of the biological effects of irradiation. However, it is believed that the amount of ROS generated from the primary ionization events are significantly lower than ROS generated from cellular metabolism[12]. Therefore, the initial production of ROS might not be entirely responsible for all cellular effects of irradiation. This observation has led to the hypothesis that ROS imbalance due to metabolic oxidative stress long after the initial radiation exposure could be an additional regulatory mechanism controlling the fate of the irradiated cell population.

A key observation of our study was the late ROS accumulation and DNA damage in SOD2 (−/−) compared to SOD2 (+/+) MEFs, correlating with an increase in transformation frequency (Figures 2–4, Tables 1 and 2). Cellular redox environment was assessed by flow cytometry measurements of DHE and DCFH-oxidation in time matched control and irradiated MEFs. Initially, there was no significant difference in cellular ROS levels among all 3 cell types compared to their respective un-irradiated control at 24 h post-IR (Figure 3A&B). The absence of any significant changes in cellular ROS levels during 24 h post-irradiation is comparable to our previously published results[6, 14]. In our previous report, we used electron paramagnetic resonance spectroscopy to measure superoxide steady state levels in 6 Gy irradiated control and SOD2 overexpressing human oral squamous carcinoma cells. These results showed no significant change in ROS levels in irradiated control compared to SOD2 overexpressing cells within hours of the radiation treatment[6]. Likewise, measurements of DHE-oxidation in irradiated SOD1 overexpressing human glioma cells were comparable to irradiated SOD1 wild-type cells during 1–5 h post-IR[14]. While the earlier results were obtained using cancer cells, results from the present study showed similar effects in normal cells, suggesting that the initial changes in cellular ROS levels immediately following the IR exposure could be independent of cellular transformation state and antioxidant enzyme activities. This notion is further supported by our results (Figure 4, Table 2) demonstrating that the IR induced DNA damage was essentially similar in all 3 cell types within 24 h post-IR. IR exposure increased the percentage of MNBNCs significantly (~3–4 folds) at 24 h post-IR; however, there was no difference among the 3 cell types. Likewise, IR exposure substantially increased γH2AX within 15 min, peaked at 30 min, and decreased by 60 min post-IR in all 3 cell types (Figure 4C). These results indicate that the IR induced early effects on cellular ROS levels and DNA damage are essentially similar among SOD2 (+/+), SOD2 (+/−), and SOD2 (−/−) MEFs.

However, IR induced late effects on cellular ROS levels and DNA damage could differ depending upon the antioxidant capacity of the cell. This “metabolic redox-response” to radiation exposures could determine the fate of the redox-sensitive cellular processes in irradiated cells. This hypothesis is supported by an earlier report demonstrating an increase in the pentose cycle activity in irradiated cells, which is believed to provide NADPH required for repair and biosynthetic processes[44]. Furthermore, an earlier report by Petkau *et al*.[7] showed that administration of SOD1 2–4 h post-IR protected Swiss mice from radiation induced lethality. Likewise, antioxidant manipulations long after the initial radiation exposures have been shown to suppress radiation induced late effects[13]. In these previously published reports,

the evidence for IR induced late effects on cellular ROS levels and DNA damage were indirect, and primarily based on the observations of elevated levels of oxidized products including 4-hydroxynonenal, 8-hydroxy-2′-deoxyguanosine, and malondialdehyde[13, 45, 46]. Our results showed a significant increase in cellular ROS levels in SOD2 (−/−) compared to SOD2 (+/+) MEFs at 72 h post-IR (Figure 3). Consistent with this increase in cellular ROS levels, the percentage of micronuclei remained higher in SOD2 (−/−) *vs.* SOD2 (+/+) MEFs (Figure 4, Table 2). Because the late ROS accumulation and percentage of micronuclei (DNA damage) were suppressed in SOD2 (+/+) compared to SOD2 (−/−) MEFs, and SOD2 activity is well known to scavenge mitochondria generated superoxide, our results indicate that mitochondria generated superoxide-signaling could regulate IR induced late effects in MEFs.

SOD2 activity and therefore mitochondria derived superoxide-signaling could influence IR induced cell cycle checkpoint activation. IR exposures are known to cause cell cycle arrest in G_1, S, and/or G_2 to prevent replication of damaged DNA or to prevent aberrant cell division. The regulatory mechanisms are known as checkpoints, and their primary function is to delay progression until the cells have adequately repaired the damage. While the IR induced G_1-checkpoint activation was comparable in all 3 cell types (data not shown), the kinetics of the G_2-checkpoint activation differed in SOD2 (−/−) *vs.* SOD2 (+/+) MEFs (Figure 5). All three cell types showed approximately 2.5-fold increase in G_2-cells at 8 h post-IR demonstrating that the G_2-checkpoint is intact in all 3 cell types. However, exit from G_2 appears to be faster in SOD2 (+/−) and SOD2 (−/−) compared to SOD2 (+/+) MEFs at 24 h post-IR (Figure 5B). Interestingly, the fold-change in G_2 in AdSOD2 infected SOD2 (−/−) MEFs was higher than AdEmpty infected SOD2 (−/−) MEFs at 24 h post-IR (Figure 5C); this observation was comparable to irradiated SOD2 (+/+) MEFs.

In summary, mouse embryonic fibroblasts lacking SOD2 activity demonstrated approximately 5-fold higher IR induced transformation frequency compared to wild type cells. SOD2 activity, therefore mitochondria derived superoxide-signaling, did not affect cellular ROS levels and DNA damage within 24 h of irradiation (early response). However, SOD2 activity significantly suppressed IR induced late ROS accumulation and DNA damage at 72 h post-IR (late response). SOD2 activity appears to influence exit from G_2 in irradiated cells. These results suggest that long after the initial irradiation a “metabolic redox-response” regulates IR induced transformation in mouse embryonic fibroblasts. These results support the hypothesis that interventions of late ROS accumulation could be a viable redox-based countermeasure for radiation exposures.

Acknowledgments

We thank Dr. Ehab H. Sarsour for assisting with the MEFs culture, Mr. Burl E. Hess and the flow cytometry core facility for assisting with flow cytometry assays, and the Radiation and Free Radical Research Core facility supported by P30-CA086862 for assisting with the radiation experiments. Funding from NIH CA111365 (PCG), CA66081 (LWO), DE-FG02-05ER64050 (DRS), and a VA Merit Review grant (JJC) supported this work.

ABBREVIATIONS

AdSOD2	adenovirus carrying mouse manganese superoxide dismutase cDNA
AdEmpty	adenovirus carrying a plasmid control vector without any insert sequence
DCFH-DA	5-(and-6)-carboxy-2′,7′-dichlorodihydrofluorescein diacetate
DHE	dihydroethidine
GSH	glutathione
GSSG	glutathione disulfide

H_2O_2	hydrogen peroxide
MEFs	mouse embryonic fibroblasts
MN	micronuclei
MNBNCs	micronuclei containing bi-nucleated cells
NPB	nucleoplasmic bridge
$O_2^{\bullet -}$	superoxide
PI	propidium iodide
SOD	superoxide dismutase
TF	transformation frequency

References

1. Hall, EJ. Radiobiology for the radiologist. Philadelphia: Lippincott Williams & Wilkins; 2000.
2. Biaglow JE, Mitchell JB, Held K. The importance of peroxide and superoxide in the X-ray response. Int J Radiat Oncol Biol Phys 1992;22:665–9. [PubMed: 1312073]
3. Oberley LW, Lindgren LA, Baker SA, Stevens RH. Superoxide lon as the cause of the oxygen effect. Radiat Res 1976;68:320–8. [PubMed: 790446]
4. Biaglow JE, Clark EP, Epp ER, Morse GM, Varnes ME, Mitchell JB. Nonprotein thiols and the radiation response of A549 human lung carcinoma cells. Int J Radiat Biol Relat Stud Phys Chem Med 1983;44:489–95. [PubMed: 6605951]
5. Epperly MW, Epstein CJ, Travis EL, Greenberger JS. Decreased pulmonary radiation resistance of manganese superoxide dismutase (MnSOD)-deficient mice is corrected by human manganese superoxide dismutase-Plasmid/Liposome (SOD2-PL) intratracheal gene therapy. Radiat Res 2000;154:365–74. [PubMed: 11023599]
6. Kalen AL, Sarsour EH, Venkataraman S, Goswami PC. Mn-superoxide dismutase overexpression enhances G_2 accumulation and radioresistance in human oral squamous carcinoma cells. Antioxid Redox Signal 2006;8:1273–81. [PubMed: 16910775]
7. Petkau A, Chelack WS, Pleskach SD. Protection of post-irradiated mice by superoxide dismutase. Int J Radiat Biol Relat Stud Phys Chem Med 1976;29:297–99. [PubMed: 1083851]
8. St Clair DK, Wan XS, Oberley TD, Muse KE, St Clair WH. Suppression of radiation-induced neoplastic transformation by overexpression of mitochondrial superoxide dismutase. Mol Carcinog 1992;6:238–42. [PubMed: 1485915]
9. Guo G, Yan-Sanders Y, Lyn-Cook BD, Wang T, Tamae D, Ogi J, Khaletskiy A, Li Z, Weydert C, Longmate JA, Huang TT, Spitz DR, Oberley LW, Li JJ. Manganese superoxide dismutase-mediated gene expression in radiation-induced adaptive responses. Mol Cell Biol 2003;23:2362–78. [PubMed: 12640121]
10. Oberley LW, St Clair DK, Autor AP, Oberley TD. Increase in manganese superoxide dismutase activity in the mouse heart after X-irradiation. Arch Biochem Biophys 1987;254:69–80. [PubMed: 3579307]
11. Summers RW, Maves BV, Reeves RD, Arjes LJ, Oberley LW. Irradiation increases superoxide dismutase in rat intestinal smooth muscle. Free Radic Biol Med 1989;6:261–70. [PubMed: 2744576]
12. Ward JF. DNA damage as the cause of ionizing radiation-induced gene activation. Radiat Res 1994;138:85–8.
13. Robbins ME, Zhao W. Chronic oxidative stress and radiation-induced late normal tissue injury, a review. Int J Radiat Biol 2004;80:251–9. [PubMed: 15204702]
14. Gao Z, Sarsour EH, Kalen AL, Li L, Kumar MG, Goswami PC. Late ROS accumulation and radiosensitivity in SOD1-overexpressing human glioma cells. Free Radic Biol Med 2008;45:1501–9. [PubMed: 18790046]

15. Spitz DR, Azzam EI, Li JJ, Gius D. Metabolic oxidation/reduction reactions and cellular responses to ionizing radiation, a unifying concept in stress response biology. Cancer Metastasis Rev 2004;23:311–22. [PubMed: 15197331]
16. Yamanaka NY, Deamer D. Superoxide dismutase activity in WI-38 cell cultures: effects of age, trypsinization, and SV-40 transformation. Physiol Chem Phys 1974;6:95–106. [PubMed: 4369250]
17. Oberley LW, Buettner GR. Role of superoxide dismutase in cancer, a review. Cancer Res 1979;39:1141–49. [PubMed: 217531]
18. Oberley LW, McCormick ML, Sierra-Rivera E, St Clair DK. Manganese superoxide dismutase in normal and transformed human embryonic lung fibroblasts. Free Radic Biol Med 1989;6:379–84. [PubMed: 2540070]
19. Sun Y, Oberley LW, Oberley TD, Elwell JH, Sierra-Rivera E. Lowered antioxidant enzymes in spontaneously transformed embryonic mouse liver cells in culture. Carcinogenesis 1993;14:1457–63. [PubMed: 8330364]
20. Zhong W, Oberley LW, Oberley TD, St Clair DK. Suppression of the malignant phenotype of human glioma cells by overexpression of manganese superoxide dismutase. Oncogene 1997;14:481–90. [PubMed: 9053845]
21. Weydert C, Roling B, Liu J, Hinkhouse MM, Ritchie JM, Oberley LW, Cullen JJ. Suppression of the Malignant Phenotype in Human Pancreatic Cancer Cells by the Overexpression of Manganese Superoxide Dismutase. Mol Cancer Ther 2003;2:361–9. [PubMed: 12700280]
22. Zhang Y, Smith BJ, Oberley LW. Enzymatic activity is necessary for the tumor-suppressive effects of MnSOD. Antioxid Redox Signal 2006;8:1283–93. [PubMed: 16910776]
23. Oberley LW. Mechanism of the tumor suppressive effect of MnSOD overexpression. Biomed and Pharmacother 2005;59:143–8.
24. Umegaki K, Fenech M. Cytokinesis-block micronucleus assay in WIL2-NS cells, a sensitive system to detect chromosomal damage induced by reactive oxygen species and activated human neutrophils. Mutagenesis 2000;15:261–9. [PubMed: 10792021]
25. Jagetia GC, Venkatesha VA. Effect of mangiferin on radiation-induced micronucleus formation in cultured human peripheral blood lymphocytes. Environ Mol Mutagen 2005;46:12–21. [PubMed: 15795888]
26. Laurent C, Voisin P, Pouget JP. DNA damage in cultured skin microvascular endothelial cells exposed to gamma rays and treated by the combination pentoxifylline and alpha-tocopherol. Int J Radiat Biol 2006;82:309–21. [PubMed: 16782648]
27. Bakkenist CJ, Kastan MB. DNA damage activates ATM through intermolecular autophosphorylation and dimer dissociation. Nature 2003;421:499–506. [PubMed: 12556884]
28. Venkatesha VA, Venkataraman S, Sarsour EH, Kalen AL, Buettner GR, Robertson LW, Lehmler HJ, Goswami PC. Catalase ameliorates polychlorinated biphenyl-induced cytotoxicity in nonmalignant human breast epithelial cells. Free Radic Biol Med 2008;45:1094–102. [PubMed: 18691649]
29. Taneja N, Davis M, Choy JS, Beckett MA, Singh R, Kron SJ, Weichselbaum RR. Histone H2AX phosphorylation as a predictor of radiosensitivity and target for radiotherapy. J Biol Chem 2004;279:2273–80. [PubMed: 14561744]
30. Fisher CJ, Goswami PC. Mitochondria-targeted antioxidant enzyme activity regulates radioresistance in human pancreatic cancer cells. Cancer Biol Ther 2008;7:1271–9. [PubMed: 18497575]
31. Sarsour EH, Venkataraman S, Kalen AL, Oberley LW, Goswami PC. Manganese superoxide dismutase activity regulates transitions between quiescent and proliferative growth. Aging Cell 2008;7:405–17. [PubMed: 18331617]
32. Reznikoff CA, Bronkow DW, Heidelberger C. Establishment and characterization of a cloned line of C3H mouse embryo cells sensitive to postconfluence inhibition of division. Cancer Res 1973;33:3231–8. [PubMed: 4357355]
33. Roti Roti JL, Malyapa RS, Bisht KS, Ahern EW, Moros EG, Pickard WF, Straube WL. Neoplastic transformation in C3H 10T(1/2) cells after exposure to 835.62 MHz FDMA and 847.74 MHz CDMA radiations. Radiation Res 2001;155:239–47. [PubMed: 11121241]
34. Sarsour EH, Agarwal M, Pandita TK, Oberley LW, Goswami PC. Manganese superoxide dismutase protects the proliferative capacity of confluent normal human fibroblasts. J Biol Chem 2005;280:18033–41. [PubMed: 15743756]

35. Griffith OW. Determination of glutathione and glutathione disulfide using glutathione reductase and 2-vinylpyridine. Anal Biochem 1980;106:207–12. [PubMed: 7416462]
36. Fenech M, Chang WP, Kirsch-Volders M, Holland N, Bonassi S, Zeiger E. HUMN project, detailed description of the scoring criteria for the cytokinesis-block micronucleus assay using isolated human lymphocyte cultures. Mutat Res 2003;534:65–75. [PubMed: 12504755]
37. Yang TCH, Tobias CA. Radiation and cell transformation *in vitro*. Adv Biol Med Phys 1980;17:417–61. [PubMed: 7457231]
38. Han A, Elkind MM. Transformation of mouse C3H/10T1/2 cells by single and fractionated doses of X-rays and fission-spectrum neutrons. Cancer Res 1979;39:123–30. [PubMed: 761182]
39. Borek C, Sachs L. In vitro cell transformation by x-irradiation. Nature 1966;210:276–78. [PubMed: 5954564]
40. Hwang BJ, Utti C, Steinberg M. Induction of cyclin D1 by submicromolar concentrations of arsenite in human epidermal keratinocytes. Toxicol Appl Pharmacol 2006;217:161–67. [PubMed: 17005224]
41. Srivastava SK, Bansal P, Oguri T, Lazo JS, Singh SV. Cell division cycle 25B phosphatase is essential for benzo(a)pyrene-7,8-Diol-9,10-epoxide induced neoplastic transformation. Cancer Res 2007;67:9150–7. [PubMed: 17909020]
42. Chen Y, Poon RY. The multiple checkpoint functions for CHK1 and CHK2 in maintenance of genome stability. Front Biosci 2008;13:5016–29. [PubMed: 18508566]
43. Zhao Y, Xue Y, Oberley TD, Kiningham KK, Lin SM, Yen HC, Majima H, Hines J, St Clair DK. Overexpression of manganese superoxide dismutase suppresses tumor formation by modulation of activator protein-1 signaling in a multistage skin carcinogenesis model. Cancer Res 2001;61:6082–8. [PubMed: 11507057]
44. Tuttle SW, Varnes ME, Mitchell JB, Biaglow JE. Sensitivity to chemical oxidants and radiation in CHO cell lines deficient in oxidative pentose cycle activity. Int J Radiat Oncol Biol Phys 1992;22:671–5. [PubMed: 1544835]
45. Kang SK, Rabbani ZN, Folz RJ, Golson ML, Huang H, Yu D, Samulski TS, Dewhirst MW, Anscher MS, Vujaskovic Z. Overexpression of extracellular superoxide dismutase protects mice from radiation-induced lung injury. Int J Radiat Oncol Biol Phys 2003;57:1056–66. [PubMed: 14575837]
46. Lonergan PE, Martin DS, Horrobin DF, Lynch MA. Neuroprotective effect of eicosapentaenoic acid in hippocampus of rats exposed to gamma-irradiation. J Biol Chem 2002;277:20804–11. [PubMed: 11912218]

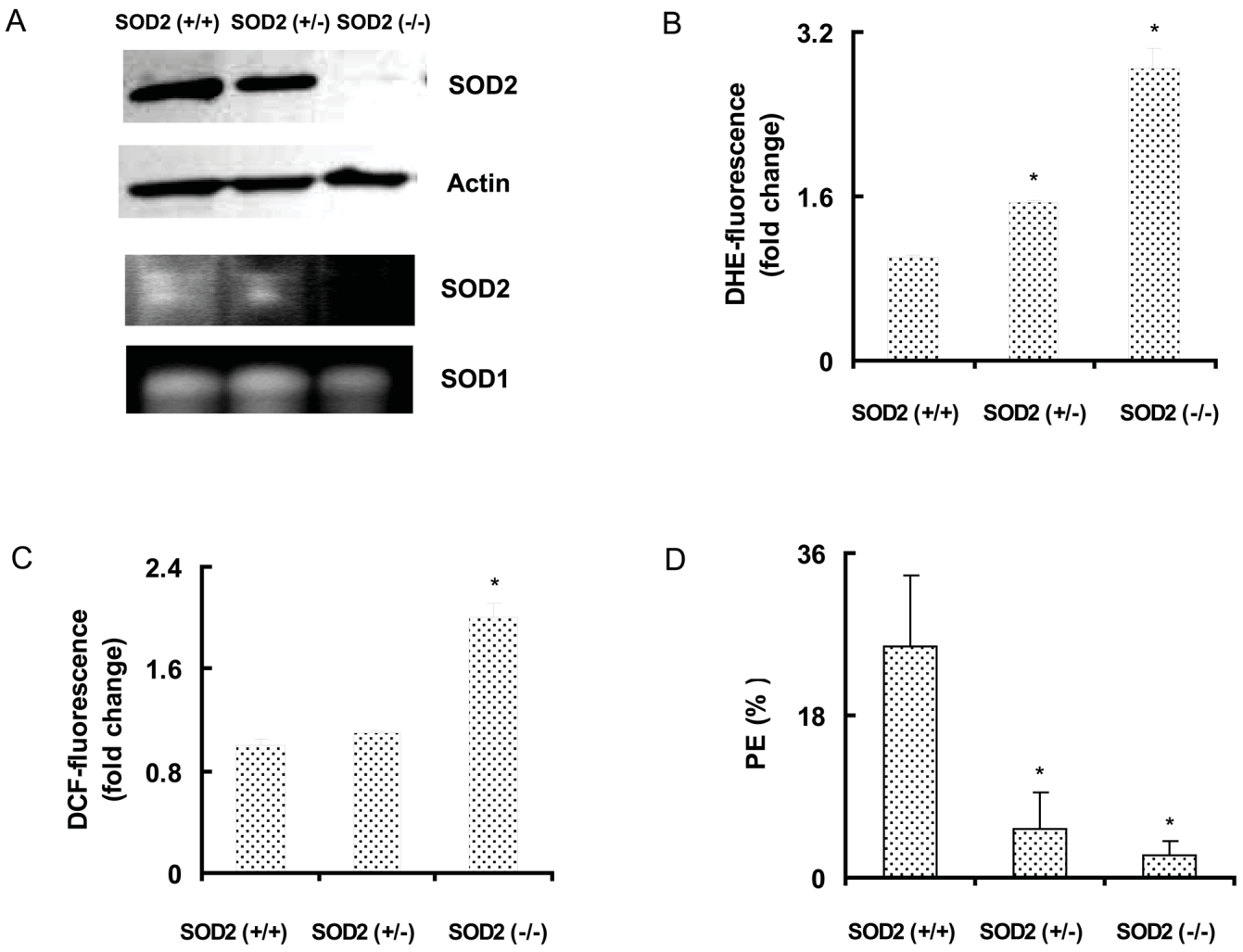

Figure 1. Cellular ROS levels and plating efficiency in SOD2 genotype mouse embryonic fibroblasts

Asynchronously growing exponential cultures of SOD2 wild type (+/+), heterozygous (+/−), and homozygous knockout (−/−) mouse embryonic fibroblasts (MEFs) were analyzed for (A) SOD2 protein and actin levels, upper two panels; bottom panels represent SOD activity analyzed by native gel-electrophoresis; flow cytometry measurements of (B) DHE and (C) DCFH-fluorescence; (D) plating efficiency; mean ± SE; * $p < 0.05$ *vs.* SOD2 (+/+).

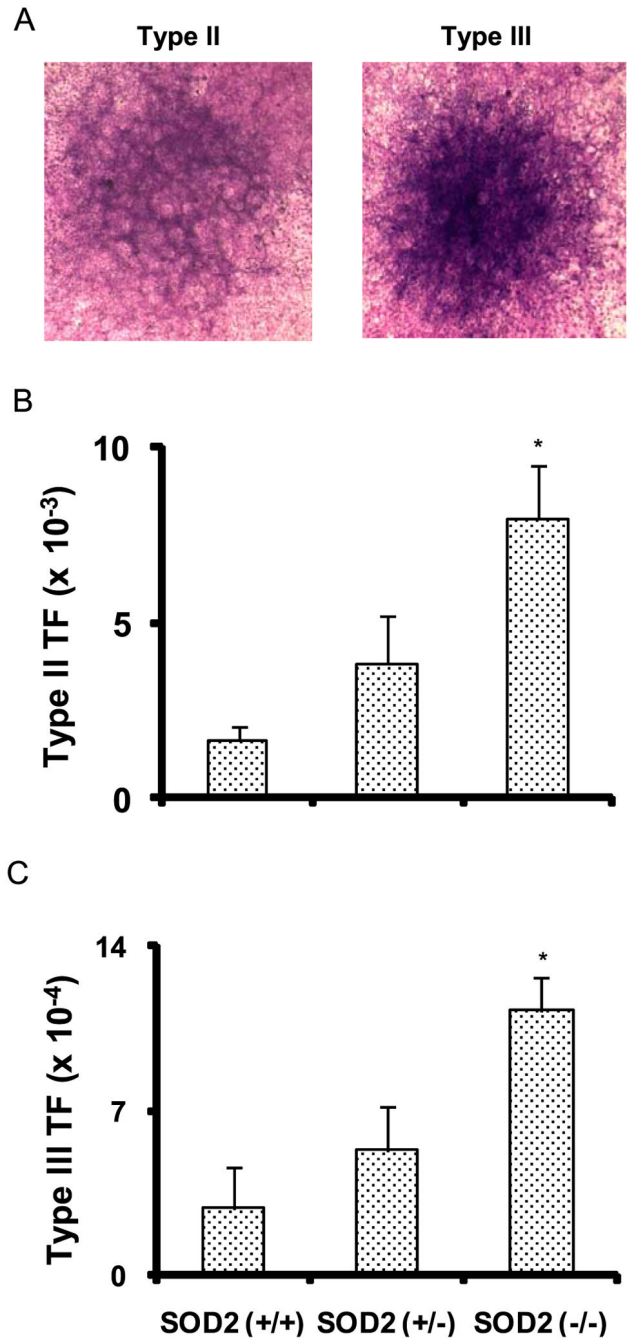

Figure 2. Increased transformation frequency in irradiated SOD2 (−/−) compared to SOD2 (+/+) MEFS

Clonogenic MEFs were seeded on 30 Gy irradiated hamster fibroblasts feeder cells, and at 24 h post-plating monolayer cultures were irradiated with equitoxic doses of ionizing radiation (dose rate, 0.83 Gy/min): 6.8 Gy for SOD2 (+/+); 4.4 Gy for SOD2 (+/−); 5.6 Gy for SOD2 (−/−) MEFs. Cells were continued in culture for 6–8 weeks; (A) representative microscopy pictures of Giemsa-stained monolayers containing Type II and III foci; transformation frequency of Type II (B) and Type III (C) foci calculated as the ratio of transformed foci relative to the number of viable cells.

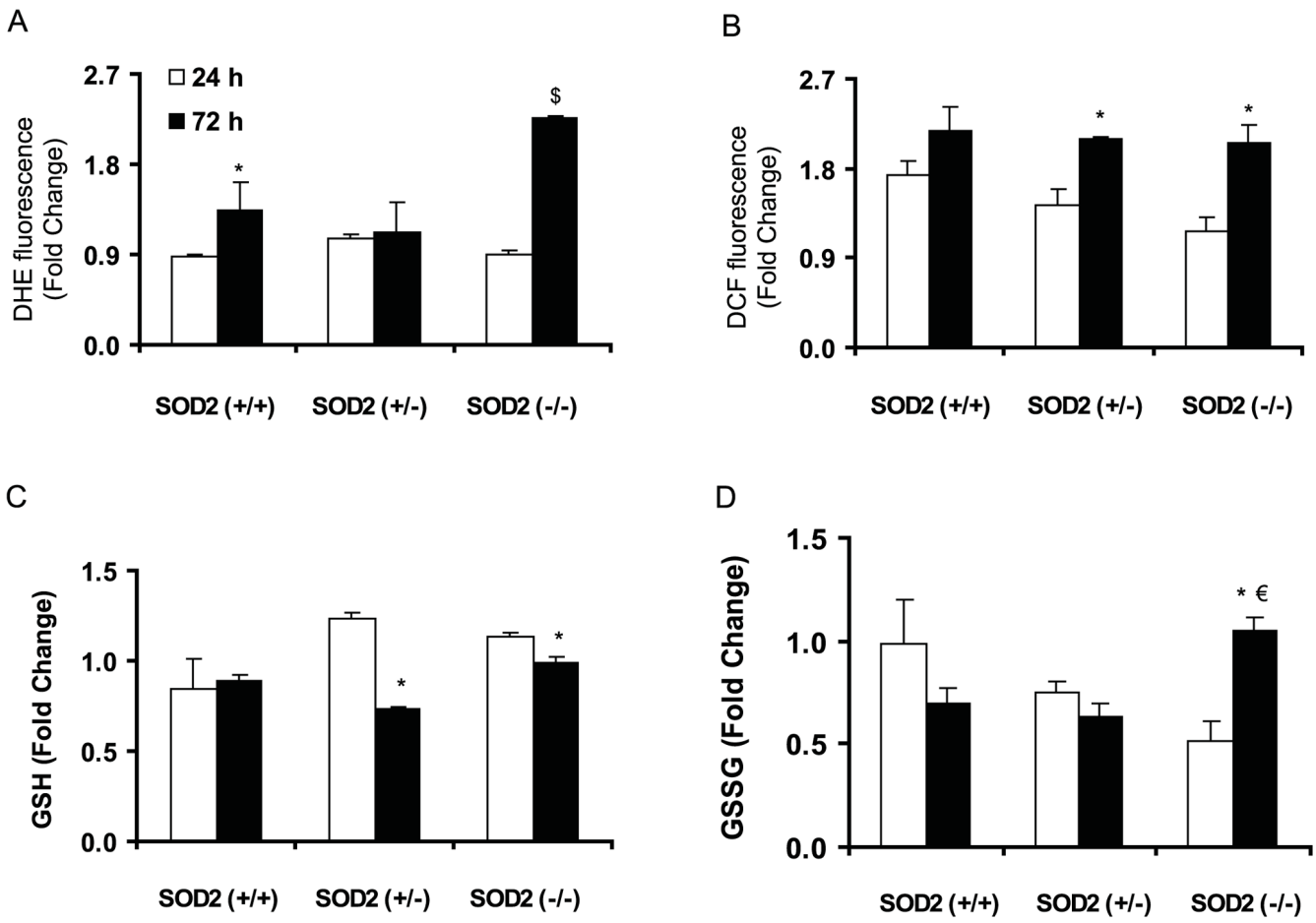

Figure 3. SOD2 activity suppressed late ROS accumulation in irradiated MEFs

Asynchronously growing exponential MEFs were irradiated with 5 Gy and harvested at indicated time for measurements of (A & B) cellular ROS levels by flow cytometry and (C & D) GSH and GSSG by biochemical assay. Fold-change was calculated relative to time matched un-irradiated cultures for each cell types: (A) DHE-fluorescence, (B) DCFH-fluorescence. * $p < 0.05$ *vs.* 24 h; €, $p < 0.05$ *vs.* SOD2 (+/+) at 72 h. Data represent mean ± SEM, n=3.

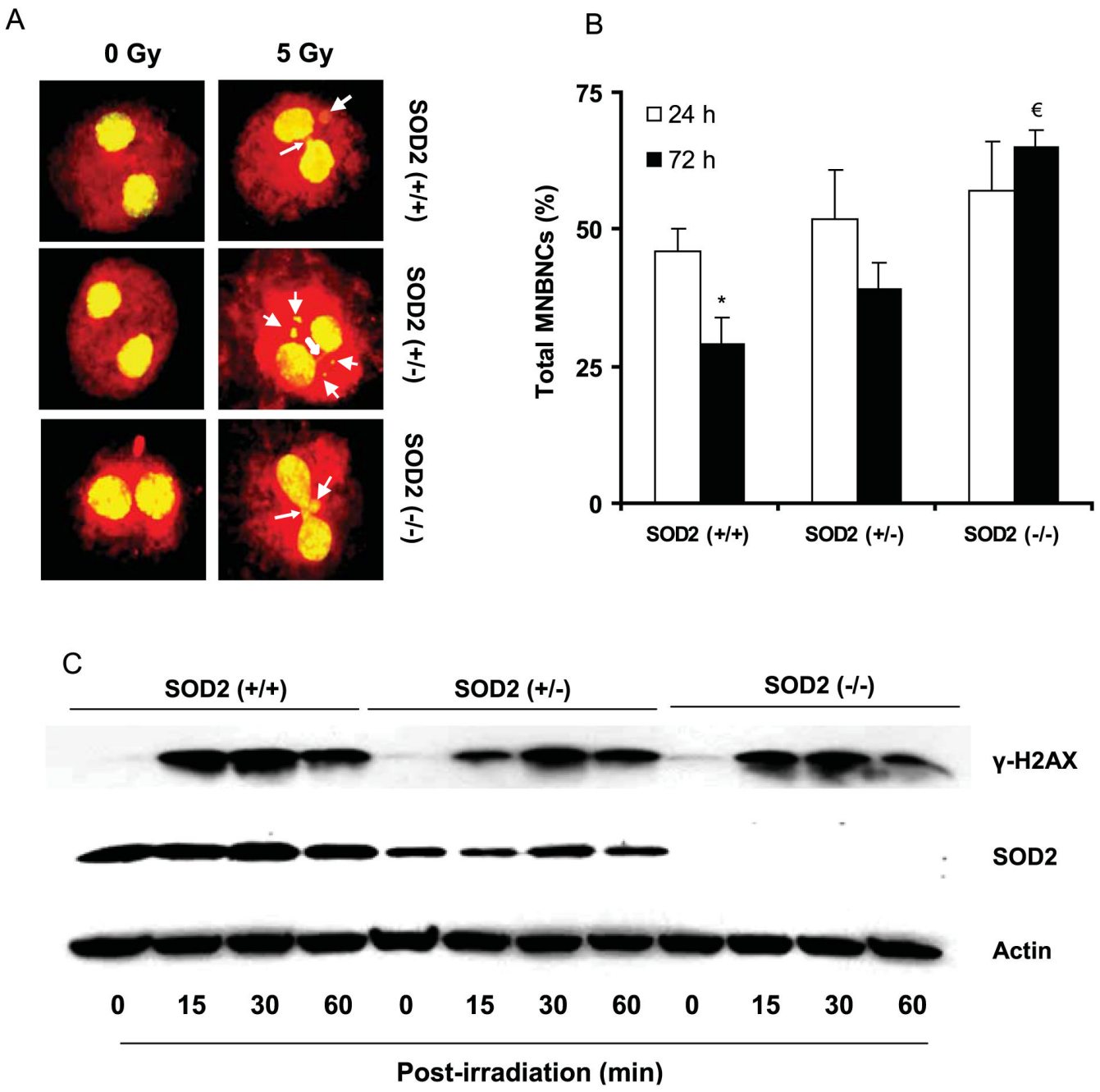

Figure 4. SOD2 activity suppressed radiation induced late DNA damage in MEFs

Asynchronously growing exponential MEFs were irradiated with 5 Gy and harvested at indicated times for measurements of DNA damage: (A) representative microscopy pictures showing micronuclei (MN) and nucleoplasmic bridge (NPB): line arrows indicate MN and solid arrows indicate NPB; (B) percentage of micronuclei bearing bi-nucleated cells (MNBNCs); *, $p < 0.05$ *vs.* SOD2 (+/+) at 24 h, and €, $p < 0.05$ *vs.* SOD2 (+/+) at 72 h post-IR. (C) Immunoblotting of γH2AX in 5 Gy irradiated MEFs.

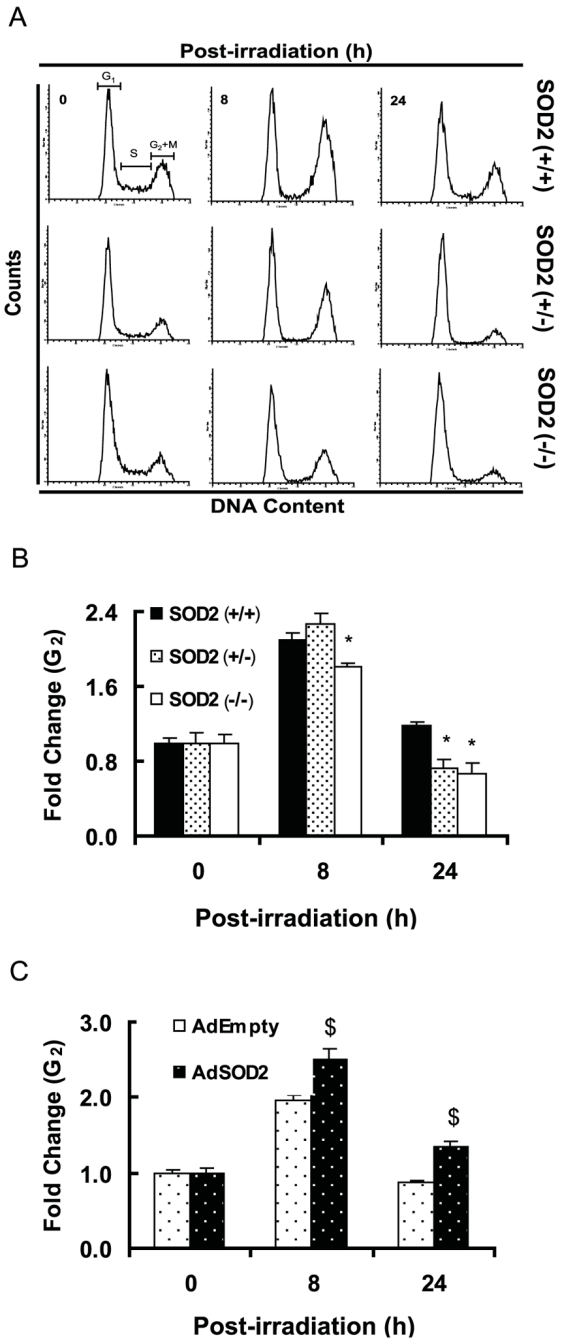

Figure 5. G_2-exit is accelerated in irradiated SOD2 (+/−) and SOD2 (−/−) compared to SOD2 (+/+) MEFs

Asynchronously growing exponential MEFs were irradiated with 5 Gy and harvested at indicated time for flow cytometry measurements of DNA content. Representative DNA histograms are shown in (A); (B) fold-change in G_2 was calculated relative to 0 h un-irradiated control for individual cell types; the percentage of G_2 in un-irradiated MEFs was as follows: SOD2 (+/+), 22%; SOD2 (+/−), 19%; SOD2 (−/−), 17%. *, $p<0.05$ *vs.* SOD2 (+/+) MEFs. (C) SOD2 (−/−) MEFs were infected with AdEmpty and AdSOD2, and irradiated with 5 Gy at 72 h post-infection. Cell cycle phase distributions analyzed at indicated times, and fold change in G_2 calculated. $, $p<0.05$ *vs.* AdEmpty infected cells.

Table 1

Increased transformation frequency in irradiated SOD2 (−/−) MEFs.

	Survival Fraction	Flasks	Total No. of Surviving Cells	No. of Foci		TF	
				Type II	Type III	Type II ($\times 10^{-3}$)	Type III ($\times 10^{-4}$)
SOD2 (+/+)	0.24	12	8611	11	2	1.28	2.32
	0.18	12	6458	10	1	1.55	1.55
	0.23	12	8285	17	4	2.05	4.83
	mean ± SEM					1.6 ± 0.4	2.9 ± 1.7
SOD2 (+/−)	0.23	12	8280	19	3	2.29	3.62
	0.17	12	6120	28	3	4.58	4.90
	0.15	12	5400	25	4	4.63	7.41
	mean ± SEM					3.8 ± 1.3	5.3 ± 1.9
SOD2 (−/−)	0.18	12	5184	33	5	6.37	9.65
	0.13	12	3432	32	4	9.32	11.67
	0.14	12	4032	33	5	8.18	12.40
	mean ± SEM					7.9 ± 1.5*	11.2 ± 1.4*

Transformation frequency (TF) of Type II = No. of Type II foci/Total surviving cells.

Transformation frequency (TF) of Type III = No. of Type III foci/Total surviving cells.

*, $p < 0.05$ *vs* SOD2(+/+) by ANOVA and Dunnett's T test.

Table 2

Percentage of BNCs containing MN in MEFs post-IR

Time (h) Post - IR	MEFs	% MNBNC (mean ± SEM)			NPB	Total MNBNCs (%)
		1 MN	2MN	3MN		
0	SOD2 (+/+)	10 ± 1.7	1 ± 1.7	0	N/A	11 ± 2.5
	SOD2 (+/−)	13 ± 2	2 ± 1	0	N/A	15 ± 1
	SOD2 (−/−)	16 ± 1	2 ± 0	0	N/A	17 ± 0.6
24	SOD2 (+/+)	27 ± 3	8 ± 3	5 ± 2	6 ± 2	46 ± 4
	SOD2 (+/−)	32 ± 5	8 ± 4	3 ± 1	9 ± 2	52 ± 9
	SOD2 (−/−)	39 ± 3	8 ± 4	3 ± 2	7 ± 2	57 ± 9*
72	SOD2 (+/+)	16 ± 2	4 ± 2	1 ± 2	8 ± 2	29 ± 5*
	SOD2 (+/−)	27 ± 6	8 ± 2	1 ± 1	4 ± 2	40 ± 5€
	SOD2 (−/−)	38 ± 5	11 ± 2	6 ± 3	11 ± 5	65 ± 3€

MNBNC, micronucleated binucleate cell; MN, micronucleus; NPB, nucleoplasmic bridge; SEM, standard error of mean. MNBNC, micronucleated binucleate cell; MN, micronucleus; NPB, nucleoplasmic bridge; SEM, standard error of mean.

*$p < 0.05$ *vs.* SOD2 (+/+) at 24 h post-irradiation and

€$p < 0.05$ *vs.* SOD2 (+/+) at 72 h post-irradiation by ANOVA and Dunnett's T test.